

# NUMERICAL ANALYSIS OF THE BEHAVIOUR OF A LARGE-DIAMETER MONOPILE FOR OFFSHORE WIND TURBINES

# NUMERIČNA ANALIZA OBNAŠANJA POSAMIČNEGA PILOTA VELIKEGA PREREZA ZA VISOKE VETRNE TURBINE

**Marx Ferdinand Ahlinhan** (*corresponding author*)  
National University of Sciences, Technologies, Eng. and Mathematics,  
Department of civil engineering  
Abomey, Republic of Benin  
E-mail: ahlinhan@yahoo.fr

**Edmond Codjo Adjovi**  
National University of Sciences, Technologies, Eng. and Mathematics,  
Department of civil engineering  
Abomey, Republic of Benin

**Valery Doko**  
University of Abomey-Calavi,  
Department of civil engineering  
Abomey-Calavi, Republic of Benin

**Herbert Nelson Tigri**  
National University of Sciences, Technologies, Eng. and Mathematics,  
Department of civil engineering  
Abomey, Republic of Benin

DOI <https://doi.org/10.18690/actageotechslov.16.1.53-69.2019>

## Keywords

offshore wind turbines, monopile, sand, combined loading, numerical modelling, loading capacity, pile-soil interaction

## Ključne besede

vetrne turbine na morju, posamični pilot, pesek, kombinirana obtežba, numerično modeliranje, nosilnost

## Abstract

*Very-large-diameter monopiles are widely used foundations for offshore wind turbines, despite the limited guidance in the codes of practice. In the present study, three-dimensional finite-element (FE) analyses were carried out to determine the static capacity of a monopile embedded in sand subjected to combined loading. A hardening soil model (HSM) accounting for the stress dependence of the soil stiffness was used for the numerical model, which was calibrated with the results of published centrifuge tests. Based on a parametric study for different length-to-diameter ratios of the monopile, lateral load-moment interaction diagrams for the ultimate limit state as well as for the serviceability limit state were developed for different relative densities of the foundation sand. Furthermore, the initial stiffness formulations for the monopile system by Carter and Kulhawy (1992), and Shadlou and Bhattacharya (2016) accounting for the effect of the pile diameter were compared to the FE results.*

## Izvleček

*Kljub omejenim smernicam v praksi se posamični piloti zelo velikega premera pogosto uporabljajo za temeljenje vetrnih turbin na morju. V tej študiji so bile izvedene tridimenzionalne analize na osnovi končnih elementov (FE) za določitev statične nosilnosti posamičnega pilota, vgrajenega v pesek, obremenjenega s kombinirano obtežbo. Za numerični model, ki je bil kalibriran z rezultati centrifugalnih testov, se je uporabil model tal z utrjevanjem (HSM), ki upošteva napetostno odvisnost od togosti tal. Na podlagi parametrične študije za različna razmerja med dolžino in premerom posamičnega pilota so bili, za različne relativne gostote peska, izdelani interakcijski diagrami bočna obtežba-upogibni moment za mejni stanji nosilnosti in uporabnosti. Narejena je bila tudi primerjava rezultatov analiz s končnimi elementi z rezultati formulacije začetne togosti sistema posamičnega pilota, ki upošteva učinek premera pilotov, avtorjev Carter in Kulhawy (1992), ter Shadlou in Bhattacharya (2016).*

## 1 INTRODUCTION

In recent decades there has been an increase in the significance of renewable energy with the aim of limiting the global temperature increase to 1.5°C with respect to the period before industrialization. This has stimulated the development of the competitive source of renewable energy, including offshore wind farms to reduce the reliance on fossil fuels and control greenhouse-gas emissions.

For offshore wind turbines there are several foundation concepts, which include monopiles, a jacket structure with four piles, a tripod with three piles, a suction caisson, a gravity base foundation, tension legs foundations, etc. The foundation design can be optimized while taking the economic and environmental optimisation issue factors into account. The cost of the foundations for offshore wind-farm developments is a significant fraction of the overall installed cost and can range from 15% to 40%, Houlsby et al. (2000) [1]. The cost-effectiveness of a particular foundation concept depends to a large extent on the site-specific conditions (water depth, soils conditions, etc.) and the power of the wind turbine. Reference can be made to Aissa et al. (2018) [2], and Kallehave et al. (2015) [3] for the applicability of each foundation structure in the function of the site-specific conditions.

Most currently used foundations are monopiles, 75% according Blanco (2009) [36] and Arshad and O'Kelly (2016) [37], and 80% according to EWEA (2015) [35] and Negro et al. (2017), [4]. Monopiles are stiff, open, steel pipe piles with a large diameter up to 8m and more, driven 30 to 45 m into the seabed with a length-to-diameter ratio ranging from 4 to 7. Fig. 1 illustrates a typical offshore wind turbine supported by a monopile foundation. The criteria for rigid or flexible behaviour have been suggested by some researchers, e.g., Dobry et al. (1982) [39] Budhu and Davies (1987) [40], and Carter and Kulhawy, 1988) [41]. According to Poulos and Hull (1989) [38] the range of transition from flexible to rigid pile behaviour can be evaluated by:

$$4.8 \leq \frac{E_{soil} L^4}{E_{pile} I_{pile}} \leq 388.6 \quad (1)$$

Based on equation 1, LeBlanc et al. (2010) [32] demonstrated that the monopile tends towards the rigid case for most sands.

The methods of analysis for pile behaviour under lateral loads range from simple empirical methods with closed-form formulae to three-dimensional finite-element methods. Reference can be made to Gurbuz (2018) [5] for the different methods of analysis for a pile under lateral loads.

The design analysis of the monopile foundation is commonly carried out based on the theory of laterally loaded piles, which relies on empirical data originating from the oil and gas industry, Reese and Matlock (1956) [6], McClelland and Focht (1958) [7], API RP (2007) [8], and DNV J 101 (2014) [9]. The lateral capacity is determined by modelling the pile as a beam column with the appropriate stiffness and the soil reaction is idealised with a system of uncoupled non-linear springs acting at discrete points along the embedded length of the monopile. This approach is known as the Winkler model. The springs are described by  $p$ - $y$  curves defining the load-displacement relationship for the interaction between the soil and the pile, API (2007) [8], DNV J 101 (2014) [9] and ISO 19901(2016) [10]. The formulation of these  $p$ - $y$  curves was originally calibrated to long slender and flexible piles with a diameter ranging from 0.34 m to 0.64 m, O'Neill et al. (1983) [11], Reese et al. (1975) [12], Reese et al. (1974) [13], and Seed et al. (1975) [14]. Furthermore, the API  $p$ - $y$  model was calibrated with the response to a small number of cycles, i.e., a maximum 200 cycles for offshore fixed-platform applications, Reese et al. (1975) [12], Reese et al. (1974) [13] and Matlock (1970) [15]. However, the monopile for offshore wind turbines behaves as a stiff pile and may undergo  $10^7$  and  $10^8$  cycles of loading over a lifetime of 20–30 years. Moreover, in the API recommendations, the initial stiffness of the  $p$ - $y$  curve is independent of the diameter of the pile, which is also questionable. In the practice, the current  $p$ - $y$  method of API can be safely applied for a pile diameter of about 2 m, without a consideration of the effect of a large pile size and the effect of a large cyclic number. These effects have to be considered for the design analysis of the typical large-diameter monopile foundation for offshore wind turbines.

To understand the behaviour of a large monopile in sand, investigations were performed in the past for both static and cyclic loading conditions, e.g., Cuellar, (2011) [16], Lesny and Wiemann (2006) [17] Sørensen (2012) [19] Abdel-Rahman et al. (2005) [20] Achmus et Thieken (2010) [21], and Achmus et al. (2013) [22]. However, the behaviour of the monopile foundation under cyclic loading is not discussed further because it is excluded from the scope of this present study. These investigations of the monopile foundation included physical modelling, numerical modelling, analytical modelling and modification of the  $p$ - $y$  curves, taking the large monopile size and the large cyclic number effects into account. Rosquet et al. (2004) [23] reported the response of a small-scale model pile under static and cyclic loading installed in sand. Centrifuge tests were performed for analysing the behaviour of the monopile in sand under monotonic and cyclic loading. Numerical and physical models of large-diameter

monopiles showed that the stiffness of the load-displacement curves increases with the monopile diameter and the common API p-y approach overestimates the initial stiffness. Therefore, the original API p-y approach underestimates the monopile deflection and overestimates the structure stiffness under the operation load, Lesny and Wiemann (2006) [15], Abdel-Rahman et al. (2005) [20], Achmus and Thieken (2010) [21], Sørensen et al. (2010) [18] Sørensen (2012) [19], and Ashford et al. (2003) [24]. The safe design analysis of a large-diameter monopile shall take the effect of the large monopile diameter and the effect of the large cyclic number into account in the case that the original API approach is applied.

Most of the above FE analyses were carried out using the Mohr-Coulomb soil model. However, the soil stiffness depends on the actual stress, and that should be considered in numerical modelling for a better understanding of the response of a monopile embedded in sand.

The main objective of this paper is to provide information for understanding the interaction soil-monopile structure for offshore wind turbines and developing conceptual interaction diagrams capable of predicting the response of a large-diameter monopile embedded in sand and subjected to combined loading. A realistic soil model that accounts for the key features of the stress-strain behaviour of sand is adopted in the FE modelling. A simplified method is also proposed for a preliminary estimation of the load capacity of the monopile in the ultimate limit state as well as in the serviceability limit state. Furthermore, the initial stiffness required for the modal analysis has been evaluated and compared with the published results in the literature.

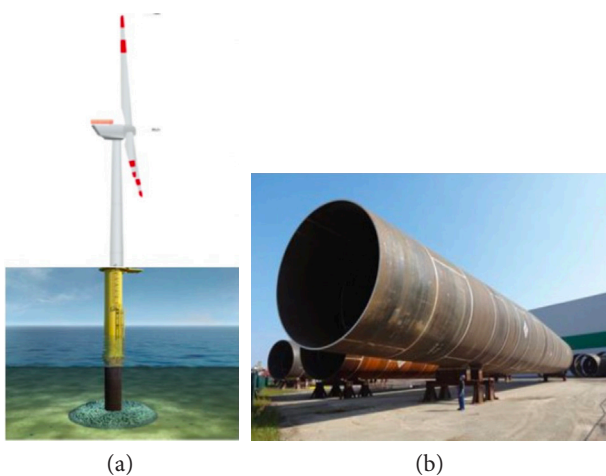


**Figure 1.** Monopile foundation system a) monopile-foundation-supported offshore wind turbine, (b) monopile structure.

## 2 FINITE-ELEMENT MODEL AND MODEL CALIBRATION

A three-dimensional finite-element model of a system consisting of the monopile and the surrounding soil was developed and analysed. The finite-element program PLAXIS 3D Foundation [25] was used for the simulations. In order to reduce the computational effort, only one half of the monopile foundation and the surrounding soil were modelled due to the symmetry of the geometrical and loading conditions. A mesh based on 15-node wedge elements, which are available in the PLAXIS 3D Foundations program [25], was applied.

Preliminary analyses were carried out for the determination of the model geometries and the mesh size in order to reach sufficient accuracy of the results and to avoid the influence of the boundary conditions. These analyses led to a soil model with a length of ten times the monopile diameter  $D$ , a soil model with a width of five times the monopile diameter  $D$ , and a soil model with a depth of 1.6 times the embedded length  $L$  of the monopile. Fig.3 shows the finite-element model with the geometric sizes.

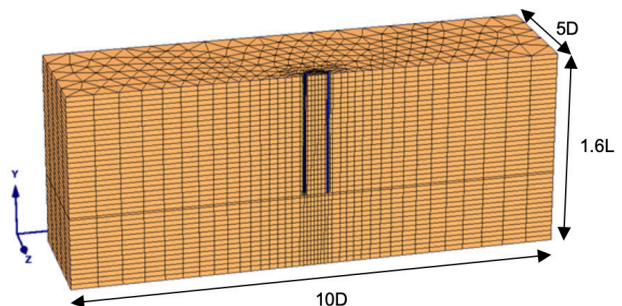


**Figure 2.** Finite-element mesh of a monopile foundation system.

Published results of field tests for a large-diameter monopile under monotonic lateral loading are scarce, since only pile tests under axial load are recommended by some design guidelines, and lateral loading tests for an offshore monopile at an offshore construction site would be very time-consuming. Therefore, back-calculations of the centrifuge tests reported in Klinkvort et al. (2011) [26], Klinkvort (2012) [27], and Rosquoet (2004) [23] were carried out for the calibration of the numerical model. Data on these centrifuge tests were also presented in Klinkvort et al. (2011) [26] Klinkvort (2012) [27], and Rosquoet (2004) [23].

Klinkvort et al. (2011) [26] and Klinkvort (2012) [27] reported the results of the centrifuge tests (Ng) for the monopile foundation under lateral loading. Their centrifuge tests were carried out on five solid steel piles

with a diameter of 16–40 mm and embedded lengths of 96–240 mm. These experimental monopiles were scaled to a prototype monopile with a diameter of  $D=1$  m and embedded length  $L=6$  m, leading to a length-to-diameter ratio of  $L/D = 6$ . The tests were performed in dry Fontainebleau sand with an average grain size  $d_{50}$  of 0.18 mm, a specific particle density of 2.65, a coefficient of uniformity  $C_u$  of 1.6, a minimum void ratio  $e_{min}$  of 0.548 and a maximum void ratio  $e_{max}$  of 0.859. The average value of the relative density is  $I_D=0.924$ , and the void ratio is  $e=0.57$ , leading to a triaxial angle of internal friction of  $\varphi=38^\circ$ .

Rosquoet (2004) [23] reported the results of the centrifuge tests for a prototype steel pile with an outer diameter of 0.72 m, an embedded length of 12 m, and a pile wall thickness of 17.5 mm. The tests were carried out with Fontainebleau sand having similar properties as described above.

For the calibration of the current numerical model, back-calculations of the tests results of Klinkvort et al. (2011) [26], Klinkvort (2012) [27], and Rosquoet (2004) [23] were carried out. The model pile geometries, soil parameters and loading conditions investigated by Klinkvort et al. (2011) [26], Klinkvort (2012) [27], and Rosquoet (2004) [23] are presented in the introduction of this paper. The load-displacement curves for the test reported by Klinkvort et al. (2011) [26], Klinkvort (2012) [27], and Rosquoet (2004) [23] were evaluated and compared with the results of the nonlinear FEM analysis in Fig. 3. It is clear that the test results and the numerical results are very comparable. Both results show a stiff behaviour of the monopile for small loads, followed by more flexible behaviour as plastic deformation occurs. The results of the

back-calculations show that the finite-element model with the nonlinear hardening soil model is able to realistically reproduce the load-displacement behaviour of a monopile foundation embedded in sand under combined monotonic loading.

### 3 PARAMETRIC STUDY AND RESULTS

Some design aspects of a monopile for wind-energy foundations include the ULS design, i.e., the proof of sufficient bearing capacity under extreme load, and the SLS design, i.e., the proof of sufficient foundation capacity under operational loads, so that the permanent rotation is lower than the value provided by the manufacturer of the wind turbines. The serviceability limit state (SLS) design for the monopile foundation for offshore wind turbines exists to show that the permanent foundation rotation does not exceed the rotation limit provided by the offshore wind turbine's manufacturer. For the offshore wind turbines installed in the North Sea, a total permanent rotation limit of  $0.5^\circ$  (including  $0.25^\circ$  for pure permanent rotation and  $0.25^\circ$  for maximum installation rotation) was often specified and applied. The performed parametric study therefore focused on the ultimate capacity and the permanent rotation of the monopile foundations. Monopile foundations with a diameter ( $D$ ) between 4 m and 8 m and with a penetration length ( $L$ ) between 16 m and 56 m were considered, leading to  $L/D$  ratios between 4 and 7 (Table 1). The wall thickness is kept constant at  $t_s=0.06$  m. The vertical load is kept constant at  $V=10$  MN, typical for a large wind turbine with a capacity of 5 MW. The simulations were carried out for dense, medium dense, loose and very loose sand, as presented in Table 2. The lateral load and the overturning moment were increased

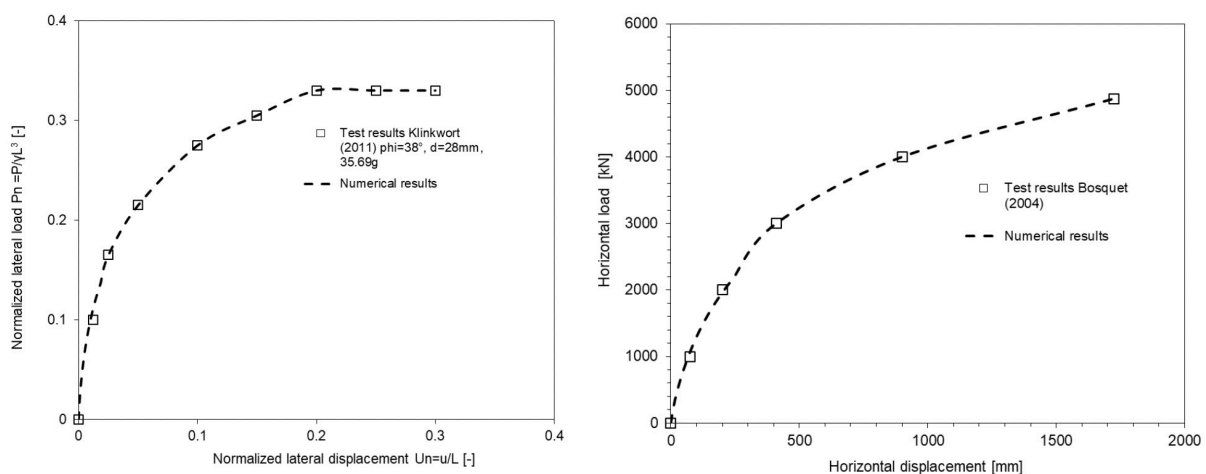
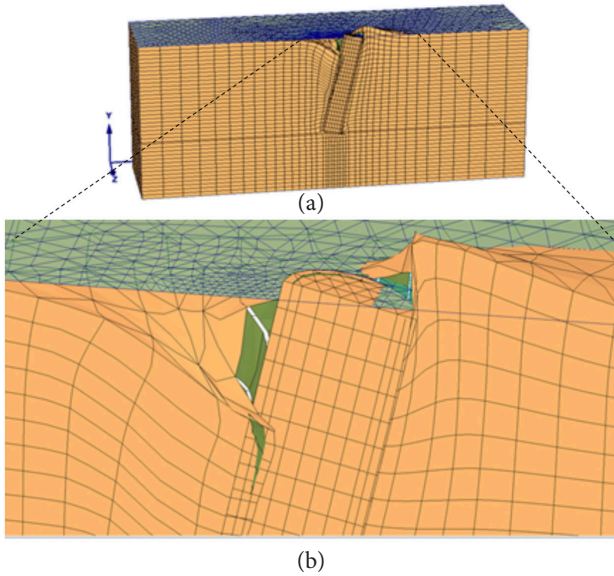


Figure 3. Comparison of the FEM and test results of Klinkvort et al. (2011) [26], Klinkvort (2012) [27], and Rosquoet (2004) [23].



**Figure 4.** Deformed finite-element mesh for reference system in failure state, a) 3D view b) 3D view up scaled.

up to the failure of the numerical model at a large lateral displacement or rotation.

**Table 1.** Monopile size considered for parametric study.

$L/D=4$	$L/D=5$	$L/D=6$	$L/D=7$
$D=4$ m; $L=16$ m	$D=4$ m; $L=20$ m	$D=4$ m; $L=24$ m	$D=4$ m; $L=28$ m
$D=5$ m; $L=20$ m	$D=5$ m; $L=25$ m	$D=5$ m; $L=30$ m	$D=5$ m; $L=35$ m
$D=6$ m; $L=24$ m	$D=6$ m; $L=30$ m	$D=6$ m; $L=36$ m	$D=6$ m; $L=42$ m
$D=7$ m; $L=28$ m	$D=7$ m; $L=35$ m	$D=7$ m; $L=42$ m	$D=7$ m; $L=49$ m
$D=8$ m; $L=32$ m	$D=8$ m; $L=40$ m	$D=8$ m; $L=48$ m	$D=8$ m; $L=56$ m

Fig. 5 presents the total deformation for the monopile foundation system. The deformation is large at the top of the monopile level and decreases with the depth to reach zero at the monopile rotation point. Fig. 6 shows the contour plot of the mobilized horizontal soil pressure for the reference system of a monopile with a diameter of 6 m and an embedded length of 30 m in medium dense sand. The horizontal soil pressure is mobilized on the passive and active side. The pressure contours formed a pressure wedge with a bulb shape around the monopile. A large horizontal soil pressure is mobilized on the passive side above the rotation point, and a small horizontal soil pressure is mobilized below

**Table 2.** Considered soil parameters for dense, medium dense, loose and very loose sand applied for the parametric study.

Parameter	Name/Unit	Dense sand	Medium dense sand	Loose sand	Very loose sand
Material model	Model	Hardening soil model	Hardening soil model	Hardening soil model	Hardening soil model
Material behaviour	Type	Drained	Drained	Drained	Drained
Effective unit weight	$\gamma'$ [kN/m <sup>3</sup> ]	9	9	8.5	8
Secant stiffness for consolidated drained triaxial test	$E_{50}$ [MN/m <sup>2</sup> ]	39	29	15	7.5
Tangent oedometer stiffness	$E_{oed}$ [MN/m <sup>2</sup> ]	39	29	15	7.5
Unloading and re-loading stiffness	$E_{ur}$ [MN/m <sup>2</sup> ]	117	87	45	22.5
Power for stress-level dependency of stiffness	$m$ [-]	0.5	0.5	0.5	0.5
Cohesion	$c$ [kN/m <sup>2</sup> ]	0.1	0.1	0.1	0.1
Effective friction angle $\varphi'$	$\varphi'$ [°]	40	36	30	25
Dilatancy angle	$\psi$ [°]	10	6	0	0
Poisson's ratio	$\nu$ [-]	0.25	0.25	0.25	0.25
Interface reduction factor	$R_{inter}$ [-]	0.60	0.61	0.63	0.64
Over-consolidation ratio	OCR [-]	1	1	1	1

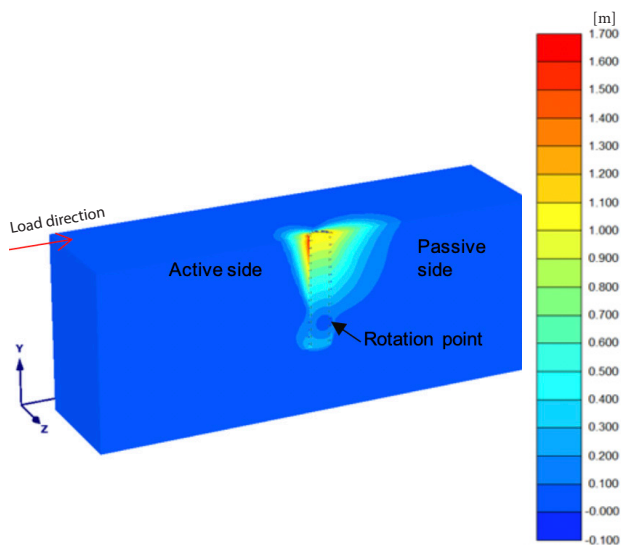


Figure 5. Contour plot of total displacement.

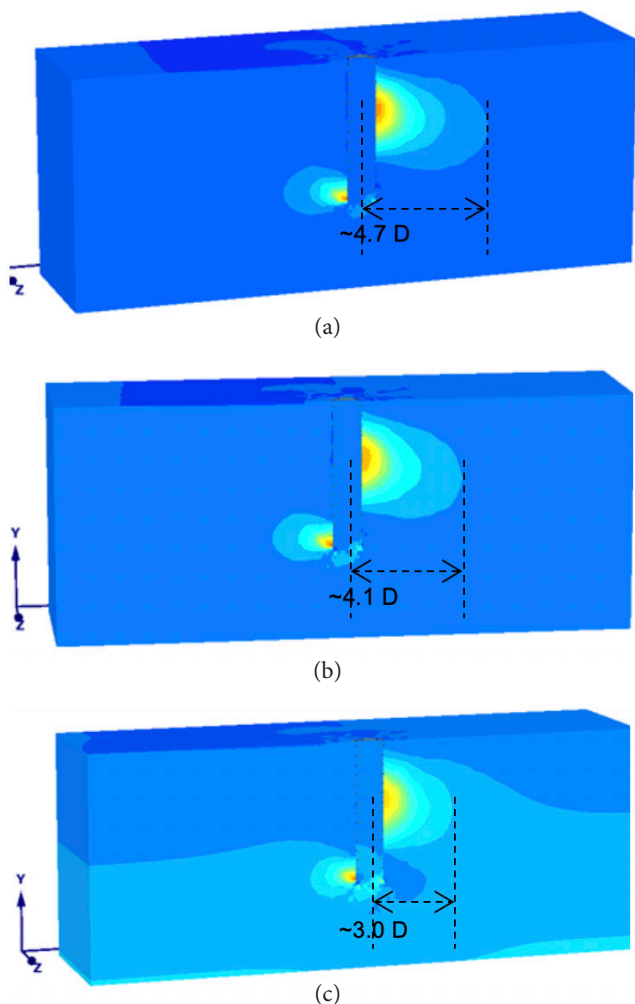


Figure 6. Contour plot of mobilized horizontal soil pressure a) dense sand b) medium dense sand c) loose sand.

the rotation point on the active side. From the horizontal soil pressure the mobilized three-dimensional passive earth pressure that resists the loading can be derived. The pressure contours generated around the monopile using the parameter study presented in Table 1 show that the horizontal earth-pressure change around the monopile extended as far as  $5.4D$  from the pile surface for single, laterally loaded, rigid, stiff piles in the failure state. This result is comparable with the value of  $6.1D$  reported by Lin et al. (2015) [28] based on the results of experimental tests with a pile diameter of 102 mm and a pile embedded length of 1.524 m using pressure sensors, and  $5.5D$  reported by Hajjalilue-Bonab et al. (2013) [29] based on the results of experimental tests with a pile diameter between 15 mm and 30 mm, and a pile embedded length between 250 mm and 550 mm using particle image velocimetry (PIV). Based on the above results a minimum lateral distance of  $12D$  between two adjacent piles is recommended in order to avoid the pile group effect due to the superimposition of the stresses. However, API RP (2007) [8] recommended a lateral distance of  $8D$  between two adjacent piles in order to avoid the pile group effect due to the superimposition of the stresses. Based on the above findings regarding the extension of the horizontal earth pressure, it can be assumed that this API recommendation might underestimate the lateral distance between large-diameter piles for the group effect analysis. Furthermore, the numerical results show the formation of a gap between the monopile and the surrounding soil located on the active side in the failure state (Fig. 4). Gapping is generally not considered as a design issue in a marine environment where sediment transport around the monopile is assumed to occur all the time and where free sand particles would migrate into any gaps formed. However, the sediment transport is influenced by many factors, including sediment type, wave- wind- and tide-induced current, the normal current, etc. Therefore, the migration of free sand particles into any gap can be considered to be a random process that should not be assumed for a robust monopile design of offshore wind turbines. Hence, the gap between the monopile and the surrounding soil should be taken into account in the design, or the possibility of the free sand migration should be analyzed based on the environmental data (sediment type, wave, wind, current, tide, etc.).

### 3.1 Ultimate capacity

The ultimate capacity of a monopile foundation in the ULS condition can be described using the force-moment interaction diagrams. Fig. 7 shows typical results of the numerical analysis in terms of the horizontal load-head

displacement ( $H-\theta$ ) and the moment–rotation ( $M-\theta$ ) relation. It can be seen that the ultimate horizontal load  $H_u=74.4$  MN and the ultimate moment  $M_u=2250$  MNm in the ULS condition.

The interaction diagrams of the ultimate capacity ( $H_u, M_u$ ) derived from numerical simulations are presented in Fig. 8 and Fig. 9. The horizontal load–moment interaction is almost linear. A similar shape of the diagrams was reported by Achmus et al. (2013) [22] for a suction bucket foundation, and Sheikh et al. (2016) [30] for a monopile with a large diameter. As expected, the monopile size and the relative density of the foundation ground significantly affect the ultimate capacity of the foundation system. The larger the monopile size, the larger the ultimate capacity is. Likewise, the larger the relative density of the foundation sand, the larger the ultimate capacity is.

Fig. 10 presents the normalized ultimate capacity. The horizontal force and overturn moment were normalized as follows:

$$\bar{M}_u = \left[ \frac{M_u}{(\gamma' \cdot L^3 \cdot D)} \right] \quad (2)$$

$$\bar{H}_u = \left[ \frac{H_u}{(\gamma' \cdot L^2 \cdot D)} \right] \quad (3)$$

The trend lines for the dense, medium dense, loose and very loose sand can be described as follows:

Dense sand:

$$\bar{H}_u = -0.98 \cdot \bar{M}_u + 2.01 \quad (4)$$

Medium dense sand:

$$\bar{H}_u = -0.93 \cdot \bar{M}_u + 1.39 \quad (5)$$

Loose sand:

$$\bar{H}_u = -0.92 \cdot \bar{M}_u + 0.81 \quad (6)$$

Very loose sand:

$$\bar{H}_u = -0.99 \cdot \bar{M}_u + 0.55 \quad (7)$$

The normalized interaction diagrams for the ultimate capacity are almost linear and parallel to each other for the considered relative densities of the foundation soil. Evidently, an estimation of the ultimate load with a deviation of 12% is possible using the equations (4) to (7), which can be applied within a scope of the preliminary design of the monopile foundation in sand for determining the monopile size for a given extreme load combination or find the ultimate load for a given monopile size. Alternatively, the non-normalized interaction diagrams in Fig. 8 and Fig. 9 can be applied for the preliminary design.

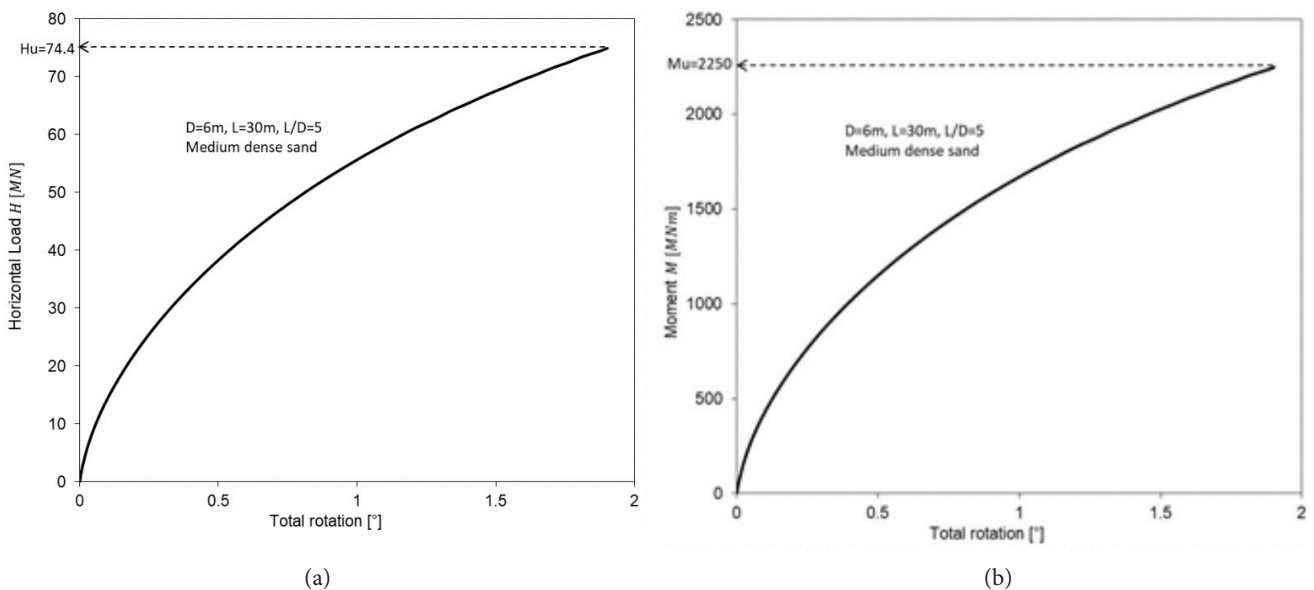


Figure 7. Typical ultimate capacity for slenderness ratios  $L/D=4$  and  $L/D=5$ , (a)  $H-\theta$  relation, (b)  $M-\theta$  relation.

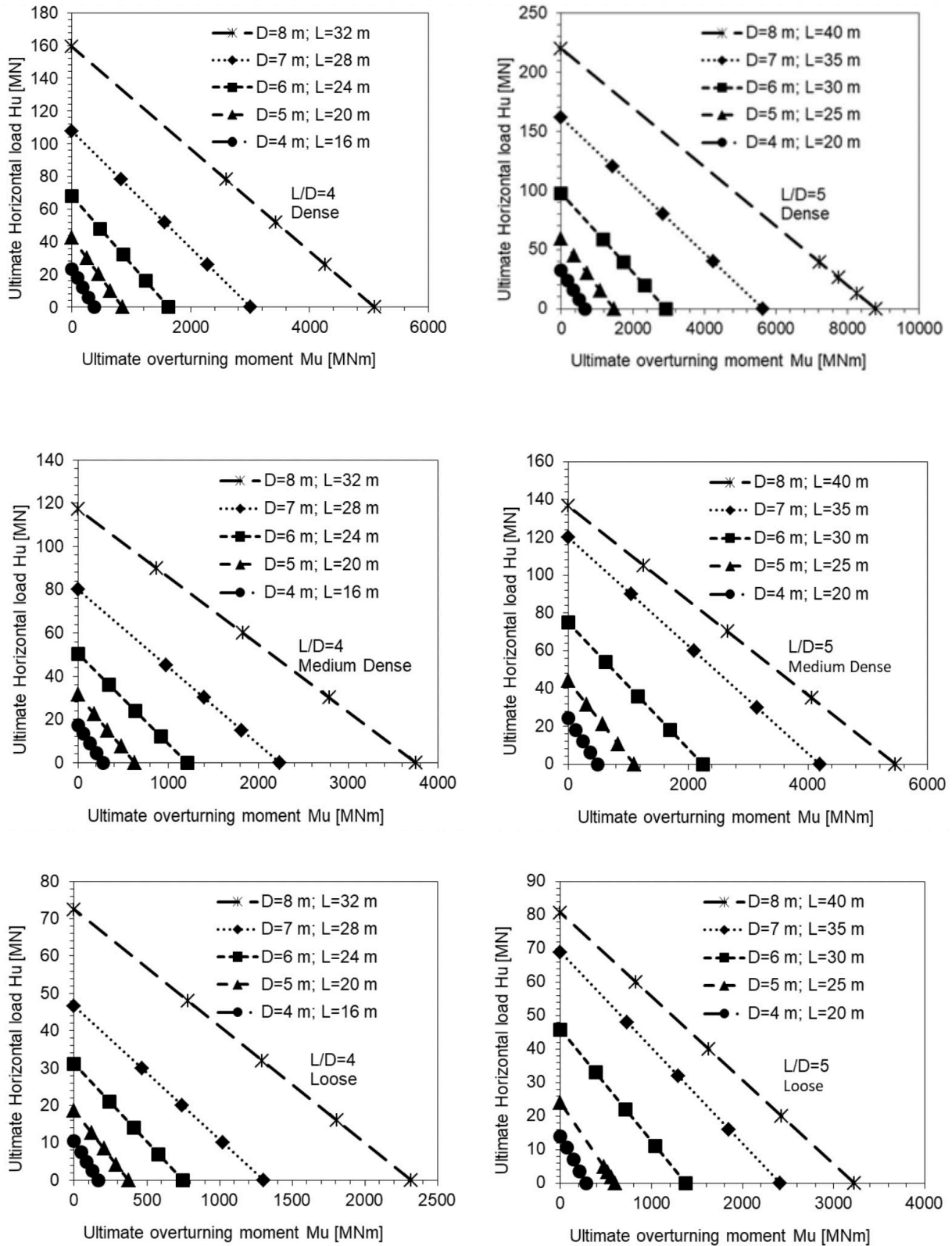


Figure 8. Ultimate capacity interaction diagrams for slenderness ratios  $L/D=4$  and  $L/D=5$ .

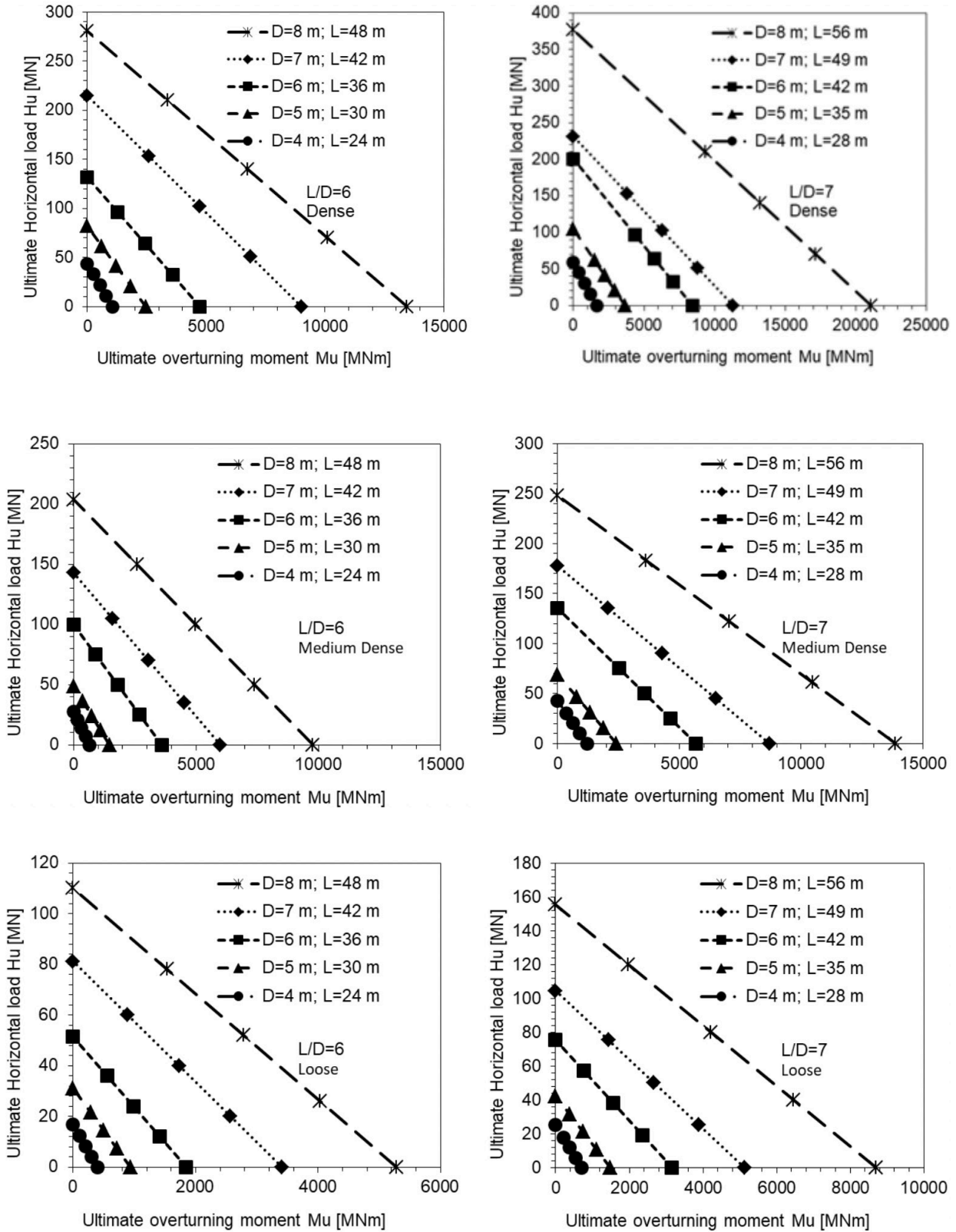


Figure 9. Ultimate capacity interaction diagrams for slenderness ratios  $L/D=6$  and  $L/D=7$ .

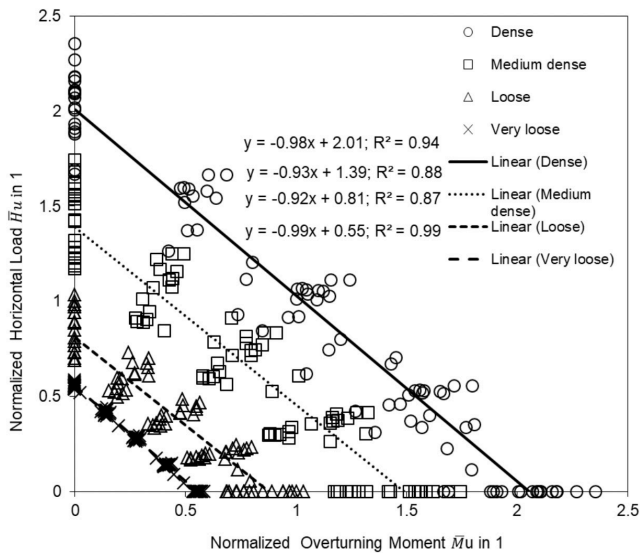


Figure 10. Normalized force moment interaction diagram for ultimate capacity.

### 3.2 Serviceability limit state

The serviceability limit state can be a governing load case for the design and the analysis of the monopile foundation for offshore wind turbines. In this case, the permanent or the plastic rotation of the monopile foundation subjected to an operating load is compared with the value provided by the wind-turbine manufacturer. A maximum permanent rotation of  $0.5^\circ$  including  $0.25^\circ$  from installation and  $0.25^\circ$  from the operation is often applied for the offshore wind turbines in the North Sea in the German sector. Fig. 11 illustrates the determination of the plastic rotation for the monopile foundation with diameter  $D=6\text{m}$ , and embedded length  $L=30\text{m}$  ( $L/D=5$ ) in medium dense sand. A straight line passing through the origin point  $O$  and a tangent to the load-rotation curve is drawn, and then a straight line parallel to this tangent passing through the failure point  $F$  intersects the  $x$ -axis by  $J$ . A straight line parallel to the  $y$ -axis passing through the failure point  $F$  intersects the  $x$ -axis by  $K$ . Per definition, the value  $OJ$  represents the plastic rotation and  $JK$  represents the elastic rotation (Fig. 11). This preliminary simplified approach is first to estimate the plastic rotation under horizontal and moment loading (one-way loading). Of course, a detailed analysis is performed in the detailed design phase where the cyclic parameters of the soil are available from advanced laboratory tests. Hereby, the cyclic loading from the wave (two-way loading) and the pore-water pressure generation and dissipation will be considered.

Fig. 12 and Fig. 13 present typical interaction diagrams for a monopile foundation in sand for a permanent rotation of  $0.25^\circ$  and  $0.50^\circ$  based on the preliminary simplified approach. Likewise, the interaction diagrams

for the normalized serviceability capacity for permanent rotations of  $0.25^\circ$ ,  $0.50^\circ$  and  $1^\circ$  are presented in Fig. 14. In this case, the normalized horizontal load and the normalized overturning moment follow the Eqs. 2 and 3. As expected, the permanent rotation increases with increasing loading and decreases with the increasing monopile size and the relative density of the foundation sand.

The approach of Zhang et al. (2005) [31] for the calculation of the ultimate lateral load capacity of a rigid pile considering both soil pressure and pile-soil interface resistance is also presented in Fig. 14. Likewise, the approach of Scheikh and Bipul (2016) [30] is presented in Fig. 14 for sand with an angle of internal friction of  $\phi' = 38.8^\circ$ , a coefficient of passive earth pressure  $k_p = 4.36$ , and a permanent rotation of  $1^\circ$ . It can be seen that the results based on the approach of Scheikh and Bipul (2016) [30] lie mainly between the numerical results for loose sand  $\phi' = 30^\circ$  and medium dense sand  $\phi' = 36^\circ$ . The results based on the approach of Zhang et al. (2005) [31] lie mainly between the numerical results for medium dense sand  $\phi' = 36^\circ$  and for dense sand  $\phi' = 40^\circ$ . Therefore, the results of the numerical analysis are comparable with the results obtained from the approach of Zhang et al. (2005) and Scheikh and Bipul (2016).

The normalized interaction diagrams for the serviceability capacity are almost linear and parallel to each other for the considered monopile size and the relative density of the soil.

These normalized interaction diagrams can be applied within the scope of the preliminary design of the monopile embedded in sand in order to determine the monopile size for a given service-load combination or to find the ultimate service load for a given monopile size. Alternatively, the non-normalized interaction diagrams in Fig. 12 and Fig. 13 can be applied for the preliminary design.

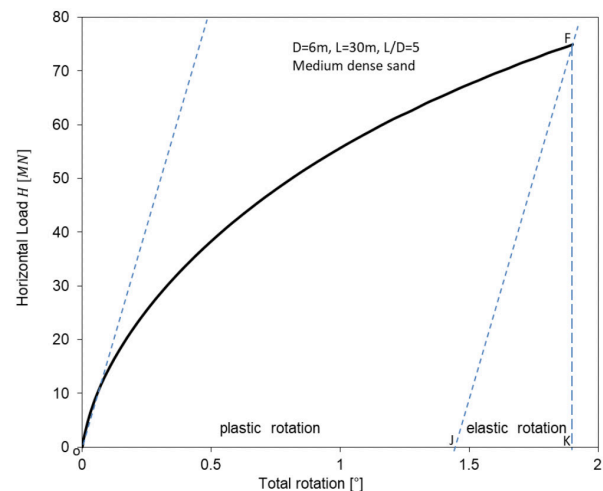


Figure 11. Determination of the plastic rotation for the reference monopile  $D=6\text{m}$ ,  $L=30\text{m}$  ( $L/D=5$ ).

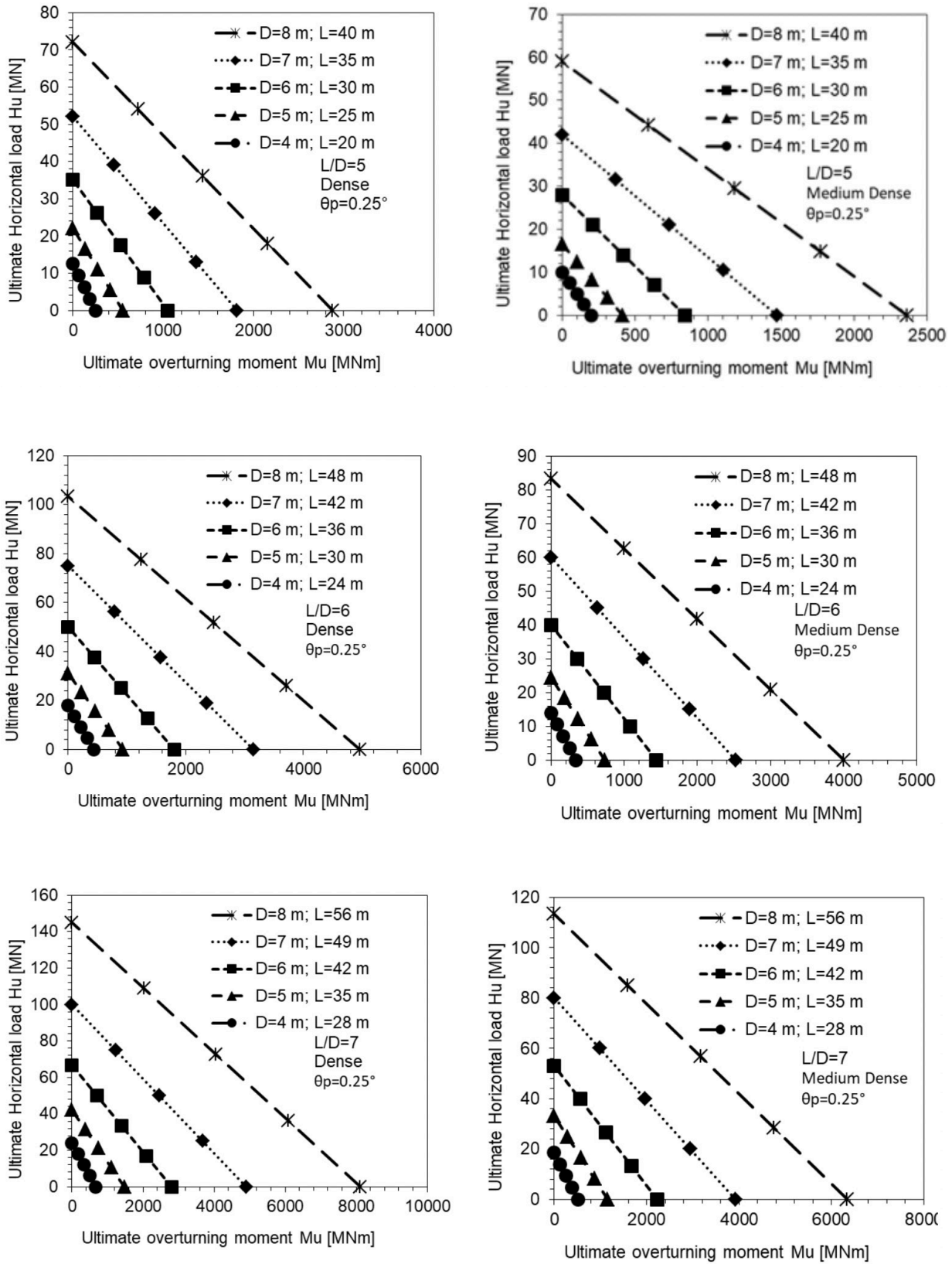


Figure 12. Force-moment interaction diagrams for permanent rotation  $\theta_p = 0.25^\circ$ .

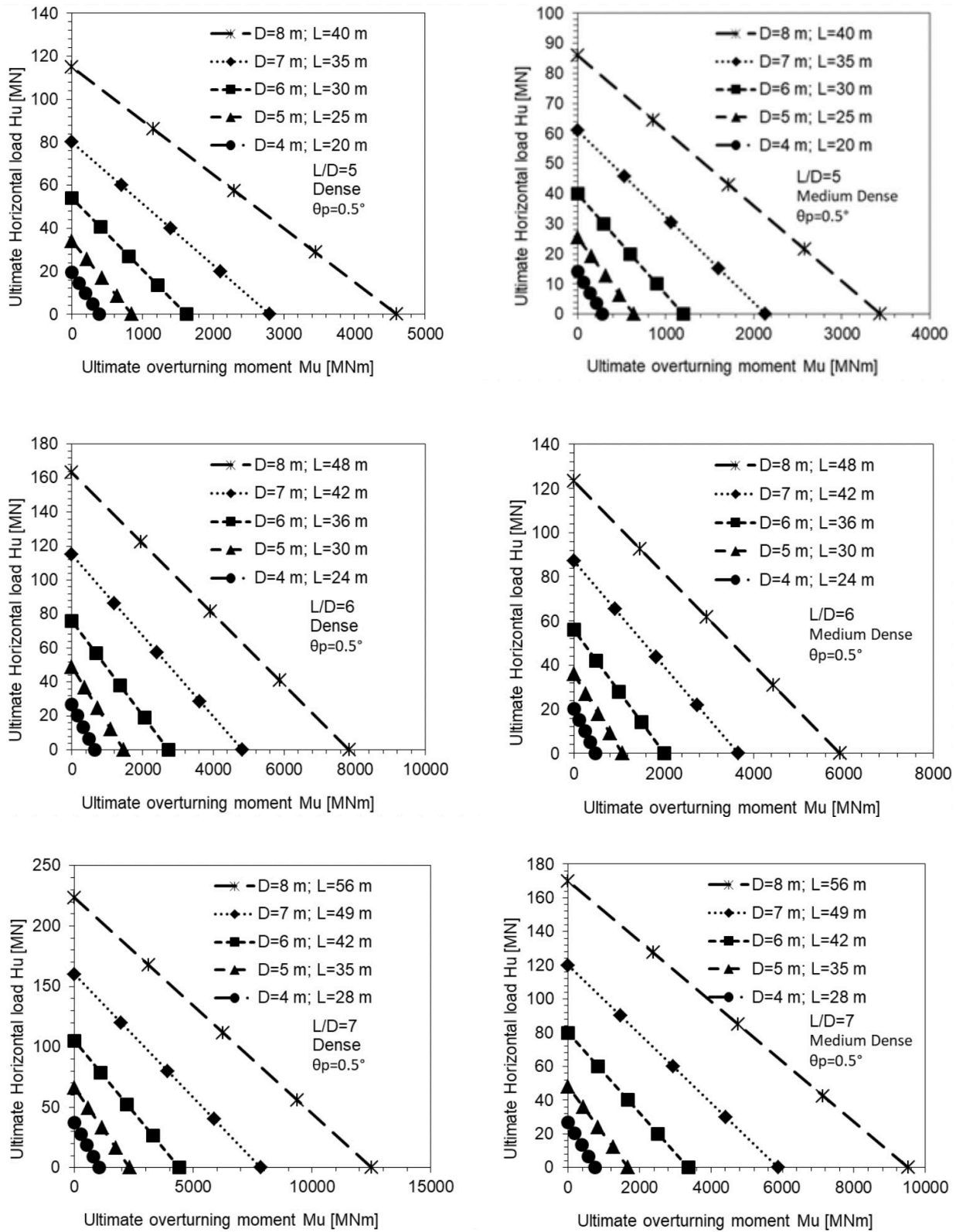


Figure 13. Force-moment interaction diagrams for permanent rotation  $\theta_p = 0.5^\circ$ .

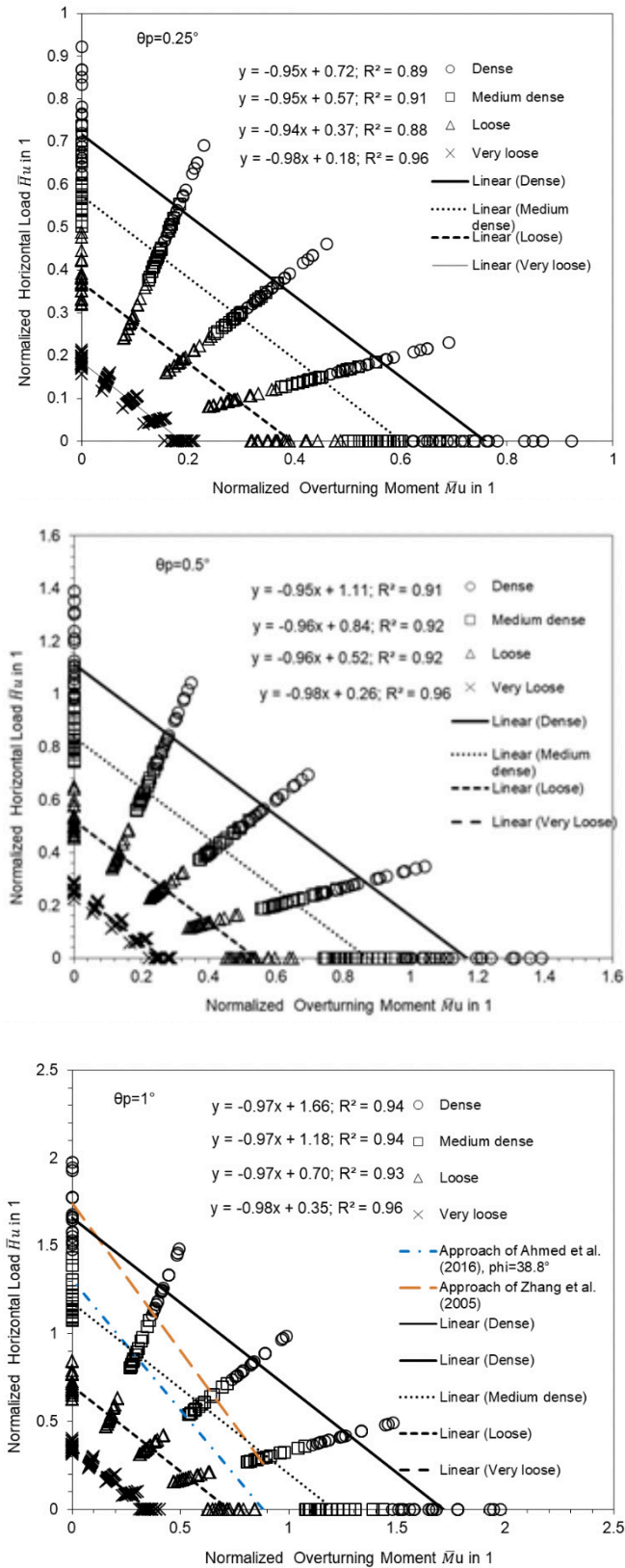


Figure 14. Normalized force-moment interaction diagrams for permanent rotation  $\theta_p=0.25^\circ$ ,  $\theta_p=0.50^\circ$  and  $\theta_p=1^\circ$ .

### 3.3 Initial stiffness

The governing design issues for offshore wind-turbine foundations include the system stiffness. An offshore wind turbine is in a permanent interaction with three media, i.e., air, water and soil. Therefore, the main sources of excitation are wind and sea waves, whereas the main source of resistance is soil associated with the structure. The wave excitation generates relatively short waves with a significant wave height  $H_s$  around 1–1.5 m and a zero-crossing period  $T_z$  around 4–5 s, Aissa et al. (2018) [2]. The excitations generated by wind are the frequencies that are in the frequencies band of the rotor rotation  $1P$  and the blade passing frequency (the blade/tower interaction), which depends on the number of blades. The blade passing frequency is often  $3P$  as most turbines currently in the market have 3 blades.  $1P$  and  $3P$  are typically in the range of 0.3 Hz and 1 Hz, respectively, Leblanc et al. (2010) [32]. The first natural frequency of an offshore wind turbine along with its substructure has a significant effect on the behaviour of the whole system. Hence, the coincidence of the tower frequency with the above-mentioned frequencies (rotor and blade passing frequencies) will lead to dynamic amplification, resulting in large stress variations in the OWT structure. This situation could potentially lead to resonance, which has to be avoided due to the fact that resonance may induce an accelerated accumulation of fatigue.

The OWT design can be performed in such a way that the first natural frequency lies within three possible ranges: an interval before the  $1P$  called the "soft-soft" region, a range after the  $3P$  known as the "stiff-stiff" region and a region located between  $1P$  and  $3P$  called the "soft-stiff" region.

In order to avoid resonance, offshore wind turbines are designed as soft-stiff, such that the first natural frequency lies between the turbine ( $1P$ ) and blade passing frequencies ( $3P$ ). The design of the structure and the substructure of an offshore wind turbine should be carried out in such a way that it sustains the permanent dynamic forces induced by vibrations during its operational life. The natural frequency of typical offshore wind turbines is influenced by the foundation stiffness. The lateral initial stiffness  $k_{hi}$ , the rotation initial stiffness  $k_{\theta i}$  and the cross-coupling initial stiffness  $k_{h\theta i}$  can be distinguished. Carter and Kulhawy (1992) [33], and Shadlou and Bhattacharya (2016) [34] proposed the initial stiffness for a rigid monopile. Fig. 15 shows a comparison of the initial lateral stiffness between the results of the finite-element analysis and the approach of Carter and Kulhawy (1992) [33], and Shadlou and Bhattacharya (2016) [34]. It can be seen that the initial horizontal

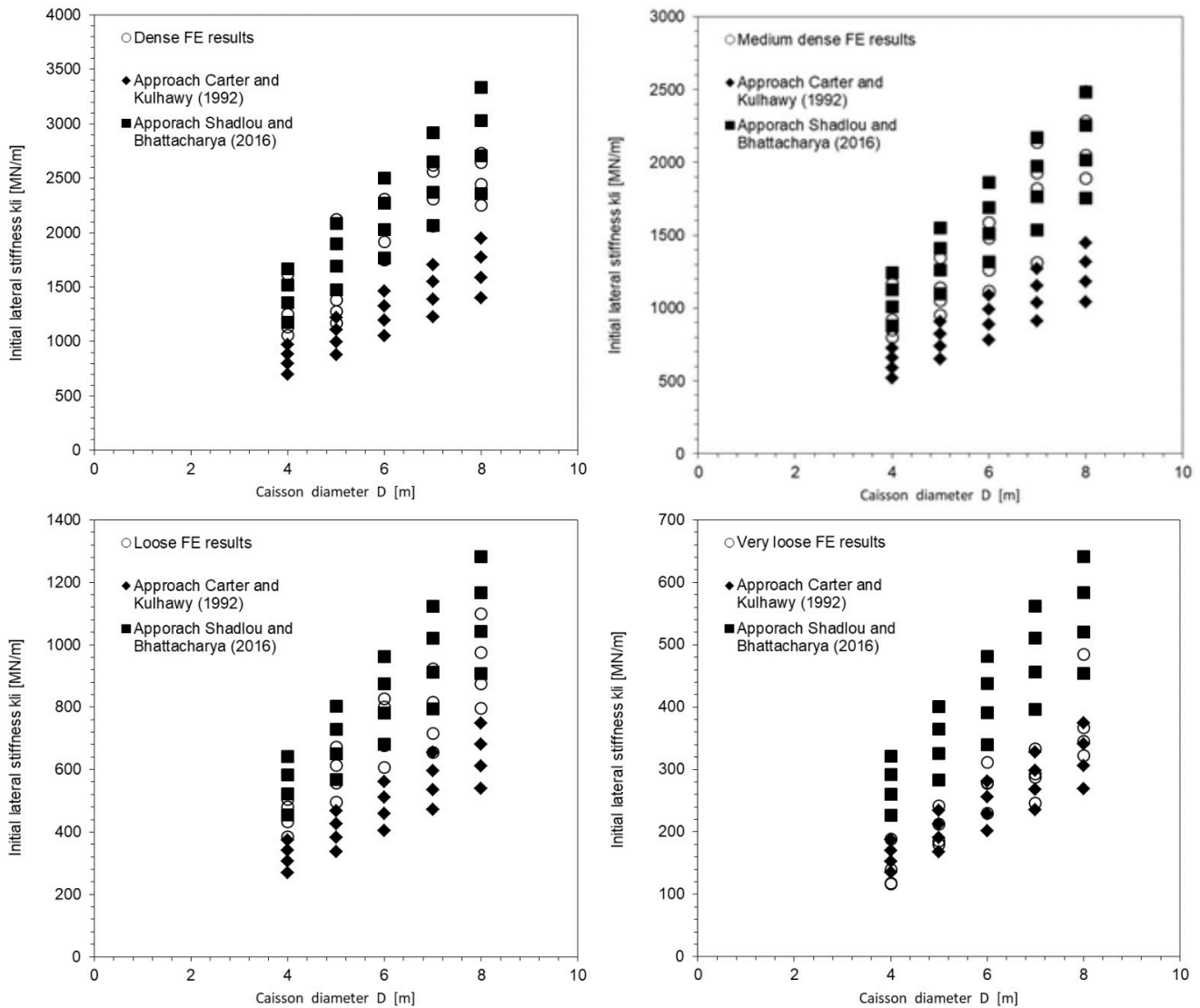


Figure 15. Comparison of initial lateral stiffness between results of a finite-element analysis and the approaches Carter and Kulhawy (1992) [33], and Shadlou and Bhattacharya (2016) [34].

stiffness is dependent on the monopile size as well as the soil stiffness. The results of the finite-element analysis are comparable with the results obtained from both the approaches. In general, the approach of Carter and Kulhawy (1992) [33] yields a slightly smaller horizontal initial stiffness than this numerical model analysis. The numerical horizontal initial stiffness and those obtained from the approach of Shadlou and Bhattacharya (2016) [34] are comparable.

#### 4 CONCLUSIONS

The monopile foundation is presently the most used foundation system for offshore wind turbines. Three-

dimensional FE analyses were carried out to investigate the behaviour of the monopile foundation in sand under combined loading ( $V=\text{constant}$ ,  $H$ ,  $M$ ). Numerical analyses were carried out by applying the Hardening Soil Model, which describes the elasto-plastic and stress-dependent behaviour of sandy soil. The following main conclusions can be drawn from the results obtained:

- The numerical back-analysis of test results reported in the literature showed that the behaviour of a monopile foundation embedded in sand under combined monotonic loading can be well reproduced by means of a numerical model using the Hardening Soil Model (HSM).
- The results of the numerical simulations showed that

the mobilized earth pressure around the monopile extended as far as  $5.4D$  from the pile surface for a single, laterally loaded, rigid, stiff pile in the failure state. This result is comparable with those reported by Li et al. (2014) [28]  $6.1D$  and by Hajialilue-Bonab et al. (2013) [29]  $5.5D$ . Therefore, it is recommended to have a lateral distance larger than  $12D$  between two adjacent piles in order to avoid the pile-group effect due to the superimposition of the stresses.

- The results of the numerical simulations showed the formation of a gap between the monopile and the surrounding soil on the active side for the condition of ultimate loading. A robust design should quantify the effect of this gap on the monopile behaviour and take this into account.
- In the ultimate loading condition the depth of the monopile rotation point ranges from approximately  $0.55L$  to  $0.65L$  ( $L$  is the embedded length of the monopile) for a monopile foundation used for an offshore wind turbine.
- With respect to the load-bearing capacity, the SLS design of the monopile foundation for the offshore wind turbine more governs the monopile design than the ULS design, due to the total permanent rotation of the monopile, generally limited to  $0.50^\circ$ .
- Numerical results for the initial lateral stiffness are comparable with the analytical results derived from the approach of Carter and Kulhawy (1992) [33], and Shadlou and Bhattacharya (2016) [34].
- The results of the parametric study showed that the ultimate capacity of the monopile foundation at ULS and SLS strongly depends on the monopile size (diameter and embedded length), the relative density and accordingly the stiffness of the foundation sand.

Normalized equations for the load-moment interaction diagrams were developed, which described the bearing capacity of the monopile foundation dependent on the embedded length ( $L$ ), the diameter ( $D$ ) of the monopile and the relative density of the foundation sand. The derived normalized interaction diagrams and equations are appropriate tools for the preliminary design of the monopile foundation for offshore wind-energy turbines in drained sand under combined monotonic loading at ULS and SLS. The findings of this numerical study are interesting and useful, but some aspects of the monopile behaviour, which are not considered here, still need further investigation. These aspects include the installation effect on the surrounding soil, the effect of cyclic loading with pore-water accumulation and dissipation, the ageing effect, etc. Therefore, further research on monopile behaviour is still needed.

## REFERENCES

- [1] Houslyby, G.T., Byrne, B.W. 2000. Suction caisson foundations for offshore wind turbines and anemometer. *Wind Engineering* 24(4), 249-255. <https://doi.org/10.1260/0309524001495611>
- [2] Aissa, M.H., Bouzid, D.A., Bhattacharya, S. 2018. Monopile head stiffness for serviceability limit state calculations in assessing the natural frequency of offshore wind turbines. *International Journal of Geotechnical Engineering* 12(3), 267-283. <https://doi.org/10.1080/19386362.2016.1270794>
- [3] Kallehave, D., Byrne, B.W., LeBlanc Thilsted C., Mikkelsen, K.K. 2015. Optimization of monopiles for offshore wind turbines. *Phil. Trans. R. Soc.* A373: 20140100.
- [4] Negro, V., López-Gutiérrez, J.S., Esteban, M.D., Alberdi, P., Imaz, M., Serracarla, J.M. 2017. Monopiles in offshore wind: Preliminary estimate of main dimensions. *Ocean Engineering* 133, 253-261. DOI: 10.1016/j.oceaneng.2017.02.011
- [5] Gurhuz, A. 2018. Modified coefficient of subgrade reaction to laterally loaded piles. *Acta Geotechnica Slovenica* 15(1), 77-85. DOI <https://doi.org/10.18690/1854-0171.15.1.77-85.2018>
- [6] Reese, L.C., Matlock, H. 1956. Non-dimensional solutions for laterally-loaded piles with soil modulus assumed proportional to depth. *Proceedings of the 8th Texas Conference on Soil Mechanics and Foundation Engineering*, Austin, Texas, 1-41.
- [7] McClelland, B., Focht, J.A., Jr. 1958. Soil modulus for laterally loaded piles. *Trans. ASCE*, ASCE, Reston, VA, 1049-1063.
- [8] API RP 2A-WSD 2007. *Planning, Designing and Constructing Fixed Offshore Platforms - Working Stress Design*, Twenty-Second Edition, American Petroleum Institute.
- [9] DNV-OS-J101 2014. *Design of Offshore Wind Turbine Structures*, DET NORSKE VERITAS AS.
- [10] ISO 19901-4 2016. *Petroleum and natural gas industries -- Specific requirements for offshore structures -- Part 4: Geotechnical and foundation design considerations*.
- [11] O'Neill, M.W., Murchison, J.M. 1983. An evaluation of p-y relationships in sands. A report to the American Petroleum Institute (PRAC 82-41-1), University of Houston-University Park, Department of Civil Engineering, Research Report No. GTDF02-83.
- [12] Reese, L.C., Cox, W.R., Koop, F.D. 1975. Field testing and analysis of laterally loaded piles in stiff clay. *Proceedings, Offshore Technology Conference*, Houston, Texas, Paper No. 2312.

- [13] Reese, L.C., Cox, W.R., Koop, F.D. 1974. Field testing and analysis of laterally loaded piles in sand. Proceedings, Offshore Technology Conference, Houston, Texas, Vol. II, Paper No.2080.
- [14] Seed, I., Makdise, B. 1975. Representation of irregular stress time histories by equivalent uniform stress series in liquefaction analyses. Report No. EERC 75-29, College of Engineering, University of California, Berkeley (USA).
- [15] Matlock, H. 1970. Correlations for design of laterally loaded piles in soft clay. Proc., 2nd Offshore Technology Conf., American Institute of Mining, Metallurgical, and Petroleum Engineers Inc., Englewood, CO, 577-594.
- [16] Cuellar, V.P. 2011. Pile Foundations for Offshore Wind Turbines: Numerical and Experimental Investigations on the Behaviour under Short-Term and Long-Term Cyclic Loading. PhD Thesis, Technical University of Berlin, 273 p.
- [17] Lesny, K., Wiemann, J. 2006. Finite-element-modelling of large diameter monopiles for offshore wind energy converters. Proceedings of Geo Congress, Atlanta, GA. ASCE, Reston, VA, 1-6.
- [18] Sørensen, S.P.H., Ibsen, L.B., Augustesen, A.H. 2010. Effects of diameter on initial stiffness of p-y curves for large-diameter piles in sand. Proceedings of the 7th European Conference on Numerical Methods in Geotechnical Engineering, 907-912.
- [19] Sørensen, S.P.H. 2012. Soil-structure interaction for non-slender, large-diameter offshore monopiles. PhD Thesis, Aalborg University Denmark, Department of Civil Engineering.
- [20] Abdel-Rahman, K., Achmus, M. 2005. Finite element modelling of horizontally loaded monopile foundations for offshore wind energy converters in Germany. Proceeding of International Symposium on Frontiers in offshore Geotechnics, Perth, Australia, 391-396.
- [21] Achmus, M., Thieken, K. 2012. Investigations the interaction relationships for piles under combined loading in cohesive and non-cohesive soils. *Geotechnik* 35 (4), 217-228 (in German).
- [22] Achmus, M., Akdag, C.T., Thieken, K. 2013. Load-bearing behaviour of suction bucket foundations in sand. *Applied Ocean Research* 43, 157-165. DOI: 10.1016/j.apor.2013.09.001
- [23] Rosquoet, F. 2004. Pieux sous charge latérale cyclique. Thèse de Doctorat, Ecole Doctorale Mécanique Thermique et Génie Civil, Ecole Centrale de Nantes, Université de Nantes, 327 p.
- [24] Ashford, S.A., Juirnarongrit, T. 2003. Evaluation of Pile Diameter Effect on Initial Modulus of Subgrade Reaction. *Journal of Geotechnical and Geoenvironmental Engineering* 129, (3), 234-242. DOI: 10.1061/(ASCE)1090-0241(2003)129:3(234)
- [25] PLAXIS, 2006. Finite Element Code for Soil and Rock Analysis, 3D Foundation Version 2.
- [26] Klinkvort, R.T., Hededal, O. 2011. Centrifuge modelling of offshore monopile foundation. *Frontiers in Offshore Geotechnics II*, ed. 1, Taylor & Francis, 581-586.
- [27] Klinkvort, R.T. 2012. Centrifuge modelling of drained lateral pile – soil response: Application for offshore wind turbine support structures. PhD Thesis, Department of Civil Engineering, Technical University of Denmark, 232 p.
- [28] Lin, H., Ni, L., Suleiman, M.T., Raich, A. 2014. Interaction between Laterally Loaded Pile and Surrounding Soil. *Journal of Geotechnical and Geoenvironmental Engineering* 141(4). [https://doi.org/10.1061/\(ASCE\)GT.1943-5606.0001259](https://doi.org/10.1061/(ASCE)GT.1943-5606.0001259)
- [29] Hajjalilue-Bonab, M., Sojoudi, Y., Puppala, A.J. 2013. Study of strain wedge parameters for laterally loaded piles. *Int. J. Geomech.* 13(2), 143-152. DOI: 10.1061/(ASCE)GM.1943-5622.0000186
- [30] Sheikh, S.A., Bipul, H. 2016. Numerical analysis of large-diameter monopiles in dense sand supporting offshore wind turbines. *International Journal of Geomechanics* 16 (5). DOI: 10.1061/(ASCE)GM.1943-5622.0000633
- [31] Zhang, L., Silva, F., Grimala, R. 2005. Ultimate lateral resistance to piles in cohesionless soils. *Journal of Geotechnical and Geoenvironmental Engineering*, 131(1), 78-83.
- [32] LeBlanc, C., Houlsby, G.T., Byrne, B.W. 2010. Response of stiff piles in sand to long-term cyclic lateral loading. *Géotechnique* 60(2), 79-90. DOI: 10.1680/geot.7.00196
- [33] Carter, J.P., Kulhawy, F.H. 1992. Analysis of laterally loaded shafts in rock. *ASCE Journal of Geotechnical Engineering* 118(6), 839-855.
- [34] Shadlou, M., Bhattacharya, S. 2016. Dynamic stiffness of monopiles supporting offshore wind turbine generators. *Soil Dynamics and Earthquake* 88, 15-32.
- [35] EWEA 2015. The European offshore wind industry - key trends and statistics 2014. January 2015: Available at: <http://www.ewea.org/fileadmin/files/library/publications/statistics/EWEA-European-Offshore-Statistics-2014.pdf> (Accessed: 23th October 2018)
- [36] Blanco, M.I. 2009. The economics of wind energy. *Renewable and Sustainable Energy Reviews* 13(6-7), 1372-1382. <https://doi.org/10.1016/j.rser.2008.09.004>
- [37] Arshad, M., O'Kelly, B. 2016. Analysis and design of monopile foundations for offshore wind turbine structures. *Marine Geosciences and Geotechnol-*

- ogy 34, 503-525. <https://doi.org/10.1080/1064119X.2015.1033070>.
- [38] Poulos, H., Hull, T. 1989. The role of analytical geomechanics in foundation engineering. In *Foundation engineering: Current principles and practices 2*, 1578–1606. Reston, VA:ASCE.
- [39] Dobry, R., Vincente, E., O'Rourke, M., Roesset, J. 1982. Stiffness and damping of single piles. *J. Geotech. Engng* 108(3), 439–458.
- [40] Budhu, M., Davies, T. 1987. Nonlinear analysis of laterally loaded piles in cohesionless soils. *Can. Geotech. J.* 24 (2), 289–296.
- [41] Carter, J., Kulhawy, F. 1988. Analysis and design of drilled shaft foundation socketed into rock. Project 1493-4, Final Report Cornell University, Ithaca, New York.